

CHAPTER 110

WAVE SCATTERING BY PERMEABLE AND IMPERMEABLE BREAKWATER OF ARBITRARY SHAPE

Takeshi IJIMA, Chung Ren CHOU and Yasu YUMURA
Professor, Doctor Course Student and Research Associate
Faculty of Engineering, Kyushu University, Fukuoka 812, Japan

Abstract

This paper deals with a theoretical method of calculation of the fluid motion, when a sinusoidal plane wave incidents to a permeable breakwater of arbitrary shape at constant water depth and shows that the problem for impermeable breakwater is solved as a special case of this method.

The method described here is the extension of the author's method⁽¹⁾ of solution for two-dimensional permeable breakwater by the method of continuation of velocity potentials for two different fluid regions into three-dimensional problems by means of Green functions.

Here, the analytical process of calculation is presented and as representative examples, wave height distributions and wave forces around an isolated elliptic- and rectangular breakwater are calculated and compared with experiments in wave channel.

The principle of this method is also applied to the analysis of submerged and semi-immersed fixed cylinder and the motions of floating body of arbitrary shape.

Introduction

We have many investigations on wave scattering problem for impermeable, straight breakwater, but few of permeable one, especially, of arbitrary shape.

Here, we show a method of calculation for fluid motion around as isolated permeable and impermeable breakwater of arbitrary shape.

Assuming the fluid resistance to be proportional to the fluid velocity, the fluid motion in a permeable breakwater regions has a velocity potential. And the motion in outer region of breakwater has also another velocity potential. These velocity potentials are developed into infinite series of orthogonal functions in terms of the depth z from still water surfaces, with eigenvalues determined by free surface and bottom boundary conditions in both fluid regions.

And the coefficients of terms in these infinite series are the functions of horizontal coordinates (x,y) and satisfy Helmholtz's

equations inherent to their own eigenvalues. Hence, by Green's identity formula, these coefficients at any point (x,y) in fluid region are expressed by their boundary values and normal derivatives to the boundary. Moreover, owing to the singularity of Green functions on the boundary, the boundary values and their normal derivatives of these coefficients are related by integral equations. Then, dividing the boundary into small elements and taking the sum, these integral equations are transformed into linear summation equations, which relate the values and their normal derivatives of coefficients on the boundary.

On the other hand, by the conditions of mechanical continuities of mass and energy flux through the boundary surface induced by fluid motions in outer and inner regions, the values and normal derivatives of above coefficients for outer region are linearly related to those for inner region.

Thus, we have two kinds of linear relations between the coefficients and their normal derivatives on the boundary and by solving these equations simultaneously, we obtain the boundary values and derivatives of coefficients. Then, by Green's identity formula, the velocity potentials and so the fluid motion at any point (x,y) in both regions are completely obtained.

As for the impermeable breakwater, the velocity potential in outer region is expressed by only two terms because of identical vanishing of scattering terms in infinite series and also normal derivatives of the coefficients vanish by the kinematical condition on the boundary. Hence the coefficients are determined by only one integral equation, from which velocity potential is easily determined.

I Analysis for Permeable Breakwater

A sinusoidal plane wave of frequency $\sigma (=2\pi/T : T$ is wave period) is assumed to incident to a permeable breakwater of arbitrary shape at constant water depth h : As shown in Fig.1, the origine of coordinate system is fixed at still water surface, x and y axes are taken in horizont, and z axis is vertically upwards. The cross-section of breakwater is indicated by a closed curve D , which shows the boundary between outer and inner fluid regions. Fluid motion in outer region I is assumed to be small amplitude wave motion in ideal, incompressible fluid, and the one in inner region II to be Darcy's flow in porous material of void V with fluid resistance proportion is μ .

Then, fluid motions in both regions have velocity potential $\phi(x,y,z)\exp(-i\sigma t)$ and wave function satisfies the following Laplace's equation.

$$\frac{\partial^2 \phi}{\partial x^2} + \frac{\partial^2 \phi}{\partial y^2} + \frac{\partial^2 \phi}{\partial z^2} = 0 \quad (1.1)$$

(i) Wave function $\phi_1(x,y,z)$ in region I

The general solution of Eq.(1.1) which satisfy free surface and bottom boundary conditions and radiation condition is expressed as follows:

$$\phi_1(x,y,z) = \frac{g\zeta_0}{\sigma} [(f_0(x,y) + f_1(x,y)) \frac{\cosh k(z+h)}{\cosh kh} + \sum_{n=1}^{\infty} f_2^{(n)}(x,y) \frac{\cos k_n(z+h)}{\cos k_n h}] \quad (1.2)$$

where g is gravity acceleration and ζ_0 is the amplitude of incident wave which is given by $\zeta_i = \zeta_0 \cos[k(x \cos \omega + y \sin \omega) + \sigma t]$, where ω is the incident angle with x axis. k and k_n are roots of the following equation.

$$kh \tanh kh = -k_n h \tanh k_n h = \sigma^2 h/g \quad (1.3)$$

$f_0(x,y)$ corresponds to the incident wave potential and is expressed by the real part of the following equation.

$$f_0(x,y) = -i \exp[-ik(x \cos \omega + y \sin \omega)] \quad (1.4)$$

$f_1(x,y)$ and $f_2^{(n)}(x,y)$ are unknown functions which satisfy the following Helmholtz's equations.

$$\frac{\partial^2 f_1}{\partial x^2} + \frac{\partial^2 f_1}{\partial y^2} + k^2 f_1 = 0, \quad \frac{\partial^2 f_2^{(n)}}{\partial x^2} + \frac{\partial^2 f_2^{(n)}}{\partial y^2} - k_n^2 f_2^{(n)} = 0 \quad (1.5)$$

(ii) Wave function $\phi_2(x,y,z)$ in region II

Fluid motion in permeable material with void V and resistance coefficient μ is determined by wave function ϕ_2 . Fluid velocity components u_i ($i=1,2,3$) and pressure intensity p are given as follows:

$$u_i = \frac{\partial \phi_2}{\partial x_i} e^{-i\sigma t}, \quad p/\rho = i \frac{\sigma}{V} (1 + i\mu V/\sigma) \phi_2 e^{-i\sigma t} - gz \quad (1.6)$$

And $\phi_2(x,y,z)$ which satisfies free surface and bottom boundary condition is expressed as follows:

$$\phi_2(x, y, z) = \frac{g_0}{\sigma} \sum_{s=1}^{\infty} f_3^{(s)}(x, y) \frac{\cosh \bar{k}_s(z+h)}{\cosh \bar{k}_s h} \quad (1.7)$$

where \bar{k}_s are the complex roots of the following equation.

$$\bar{k}_s h \tanh \bar{k}_s h = (1 + i\mu V/\sigma) \sigma^2 h/g, \quad (s=1, 2, 3, 4, \dots) \quad (1.8)$$

$f_3^{(s)}(x, y)$ are unknown functions to satisfy next equation.

$$\frac{\partial^2 f_3^{(s)}}{\partial x^2} + \frac{\partial^2 f_3^{(s)}}{\partial y^2} + \bar{k}_s^2 f_3^{(s)} = 0 \quad (1.9)$$

(iii) Representation of f_1 , $f_2^{(n)}$, $f_3^{(s)}$ by means of Green's identity formula
 Indicating the point on the boundary D by (ξ, η) and the point in fluid region I and II by (x, y) , the distance between them is

$$r(x, y; \xi, \eta) = r(\xi, \eta; x, y) = \sqrt{(x-\xi)^2 + (y-\eta)^2} \quad (1.10)$$

Green functions which are particular solutions of Eq. (1.5) and (1.9) with singularities of order $\log r$ when r tends to zero and satisfy Sommerfeld's⁽²⁾

radiation condition when r tends to infinity are $-\frac{i}{2}H_0^{(1)}(kr)$ for f_1 , $-K_0(k_n r)/\pi$ for $f_2^{(n)}$ and $-\frac{i}{2}H_0^{(1)}(\bar{k}_s r)$ for $f_3^{(s)}$, where $H_0^{(1)}$ and K_0 are Hankel function of the first kind and modified Bessel function of order zero, respectively.

Then, following to Green's identity formula, $f_1(x, y)$, $f_2^{(n)}(x, y)$ and $f_3^{(s)}(x, y)$ are represented by their values $f_1(\xi, \eta)$, $f_2^{(n)}(\xi, \eta)$, $f_3^{(s)}(\xi, \eta)$ and their normal derivatives $\bar{f}_1(\xi, \eta) = \partial f_1(\xi, \eta)/k\partial\nu$, $\bar{f}_2^{(n)}(\xi, \eta) = \partial f_2^{(n)}(\xi, \eta)/k\partial\nu$, $\bar{f}_3^{(s)}(\xi, \eta) = \partial f_3^{(s)}(\xi, \eta)/k\partial\nu$ on the boundary D as follows:

$$f_1(x, y) = -\frac{1}{2} \int_D [f_1(\xi, \eta) \frac{\partial}{\partial\nu} (-\frac{i}{2} H_0^{(1)}(kr)) - (-\frac{i}{2} k H_0^{(1)}(kr)) \bar{f}_1(\xi, \eta)] ds \quad (1.11)$$

$$f_2^{(n)}(x, y) = -\frac{1}{2} \int_D [f_2^{(n)}(\xi, \eta) \frac{\partial}{\partial\nu} (-K_0(k_n r)/\pi) - (-k K_0(k_n r)/\pi) \bar{f}_2^{(n)}(\xi, \eta)] ds \quad (1.12)$$

$$f_3^{(s)}(x, y) = \frac{1}{2} \int_D [f_3^{(s)}(\xi, \eta) \frac{\partial}{\partial\nu} (-\frac{i}{2} H_0^{(1)}(\bar{k}_s r)) - (-\frac{i}{2} k H_0^{(1)}(\bar{k}_s r)) \bar{f}_3^{(s)}(\xi, \eta)] ds \quad (1.13)$$

where ν is outward normal to the boundary and integral is the line integral taken in counter-clockwise direction along the boundary D.

Taking the limit when point (x, y) tends to any point (ξ', η') on the

boundary, Eq. (1.11) (1.12) (1.13) give the following integral equations.

$$f_1(\xi', \eta') = - \int_D [f_1(\xi, \eta) \frac{\partial}{\partial v} (-\frac{i}{2} H_0^{(1)}(kR)) - (-\frac{i}{2} k H_0^{(1)}(kR)) \bar{f}_1(\xi, \eta)] ds \quad (1.14)$$

$$f_2^{(n)}(\xi', \eta') = - \int_D [f_2^{(n)}(\xi, \eta) \frac{\partial}{\partial v} (-K_0(k_n R)/\pi) - (-k_n K_0(k_n R)/\pi) \bar{f}_2^{(n)}(\xi, \eta)] ds \quad (1.15)$$

$$f_3^{(s)}(\xi', \eta') = \int_D [f_3^{(s)}(\xi, \eta) \frac{\partial}{\partial v} (-\frac{i}{2} H_0^{(1)}(\bar{k}_s R)) - (-\frac{i}{2} k H_0^{(1)}(\bar{k}_s R)) \bar{f}_3^{(s)}(\xi, \eta)] ds \quad (1.16)$$

where $R = \sqrt{(\xi' - \xi)^2 + (\eta' - \eta)^2}$

(iv) Transform of line integral to summation

Dividing the boundary curve D into small N segments S_j ($j=1, 2, 3, \dots, N$) by N points and indicating the central point of each segment by (ξ_j, η_j) , the line integral along D is replaced by summation as follow, for example:

$$\int_D f_1(\xi, \eta) \frac{\partial}{\partial v} (-\frac{i}{2} H_0^{(1)}(kR)) ds = \sum_{j=1}^N f_1(\xi, \eta) \int_{\Delta S_j} \frac{\partial}{\partial v} (-\frac{i}{2} H_0^{(1)}(kR_{ij})) ds \quad (1.17)$$

where $R_{ij} = \sqrt{(\xi_j - \xi_i)^2 + (\eta_j - \eta_i)^2}$ and (ξ_i, η_i) is any fixed point corresponding to (ξ', η') .

Thus, Eq. (1.14) (1.15) (1.16) are written by the following summation equations.

$$f_1(i) + \sum_{j=1}^N \{ \bar{A}_{ij} f_1(j) - A_{ij} \bar{f}_1(j) \} = 0 \quad (1.18)$$

$$f_2^{(n)}(i) + \sum_{j=1}^N \{ \bar{B}_{ij}^{(n)} f_2^{(n)}(j) - B_{ij}^{(n)} \bar{f}_2^{(n)}(j) \} = 0 \quad (1.19)$$

$$f_3^{(s)}(i) - \sum_{j=1}^N \{ \bar{E}_{ij}^{(s)} f_3^{(s)}(j) - E_{ij}^{(s)} \bar{f}_3^{(s)}(j) \} = 0 \quad (1.20)$$

where $f_1(j)$, $\bar{f}_1(j)$, etc. represent $f_1(\xi_j, \eta_j)$, $\bar{f}_1(\xi_j, \eta_j)$, etc. and

$$A_{ij} = \int_{\Delta S_j} (-\frac{i}{2} k H_0^{(1)}(kR_{ij})) ds, \quad \bar{A}_{ij} = \int_{\Delta S_j} \frac{\partial}{\partial v} (-\frac{i}{2} H_0^{(1)}(kR_{ij})) ds$$

$$B_{ij}^{(n)} = \int_{\Delta S_j} (-k_n K_0(k_n R_{ij})/\pi) ds, \quad \bar{B}_{ij}^{(n)} = \int_{\Delta S_j} \frac{\partial}{\partial v} (-k_n K_0(k_n R_{ij})/\pi) ds$$

$$E_{ij}^{(s)} = \int \Delta S_j (-\frac{i}{2} k H_0^{(1)}(\bar{k}_s R_{ij})) ds, \quad \bar{E}_{ij}^{(s)} = \int \Delta S_j \frac{\partial}{\partial v} (-\frac{i}{2} H_0^{(1)}(\bar{k}_s R_{ij})) ds \quad (1.21)$$

$$R_{ij} = \sqrt{(\xi_j - \xi_i)^2 + (\eta_j - \eta_i)^2}$$

(v) Mechanical continuity conditions along boundary D

Mass and energy flux induced by fluid motions in inner and outer regions should be continuous through the immersed surface of breakwater. These conditions are satisfied by the continuities of fluid velocities normal to the boundary D and of the fluid pressure intensities at the boundary. Fluid pressure in outer and inner regions p_1 and p_2 are given as follows⁽³⁾:

$$p_1/\zeta = i\phi_1(x,y,z)e^{-i\sigma t}, \quad p_2/\zeta = i\sigma \frac{1+i\mu V/\sigma}{V} \phi_2(x,y,z)e^{-i\sigma t} \quad (1.22)$$

Therefore, the continuity conditions are expressed as follows:

$$\partial\phi_1(\xi,\eta,z)/\partial v = \partial\phi_2(\xi,\eta,z)/\partial v, \quad \phi_1(\xi,\eta,z) = \frac{1+i\mu V/\sigma}{V} \phi_2(\xi,\eta,z) \quad (1.23)$$

Substituting Eq.(1.2) and (1.7) into above equations, we obtain

$$(\bar{f}_0(\xi,\eta) + \bar{f}_1(\xi,\eta)) \frac{\cosh k(z+h)}{\cosh kh} + \sum_{n=1}^{\infty} \bar{f}_2^{(n)}(\xi,\eta) \frac{\cos k_n(z+h)}{\cos k_n h} = \sum_{s=1}^{\infty} \bar{f}_3^{(s)}(\xi,\eta) \frac{\cosh \bar{k}_s(z+h)}{\cosh \bar{k}_s h} \quad (1.24)$$

$$[f_0(\xi,\eta) + f_1(\xi,\eta)] \frac{\cosh k(z+h)}{\cosh kh} + \sum_{n=1}^{\infty} f_2^{(n)}(\xi,\eta) \frac{\cos k_n(z+h)}{\cos k_n h} = \frac{1+i\mu V/\sigma}{V} \sum_{s=1}^{\infty} f_3^{(s)}(\xi,\eta) \frac{\cosh \bar{k}_s(z+h)}{\cosh \bar{k}_s h} \quad (1.25)$$

Multiplying each term of above equations by $\cosh k(z+h)$ and $\cos k_n(z+h)$, and integrating from $z=-h$ to $z=0$, we have next relations.

$$f_1(\xi,\eta) = -[f_0(\xi,\eta) + \frac{\alpha}{N_0} \sum_{s=1}^{\infty} \frac{f_3^{(s)}(\xi,\eta)}{1 - (\bar{\lambda}_s/\lambda_0)^2}] \quad (1.26)$$

$$f_2^{(n)}(\xi,\eta) = -\frac{\beta}{N_n} \sum_{s=1}^{\infty} \frac{f_3^{(s)}(\xi,\eta)}{1 + (\bar{\lambda}_s + \lambda_n)^2} \quad (1.27)$$

$$\bar{F}_1(\xi, \eta) = -[\bar{F}_0(\xi, \eta) + \frac{\alpha}{N_0} \sum_{s=1}^N \frac{\bar{F}_3^{(s)}(\xi, \eta)}{1 - (\bar{\lambda}_s/\lambda_0)^2}] \quad (1.28)$$

$$\bar{F}_2^{(n)}(\xi, \eta) = -\frac{\beta}{N_n} \sum_{s=1}^N \frac{\bar{F}_3^{(s)}(\xi, \eta)}{1 + (\bar{\lambda}_s/\lambda_n)^2} \quad (1.29)$$

$$\alpha = i\frac{h}{\sigma}(1 + i\nu V/\sigma), \quad \beta = i\nu V/\sigma, \quad \lambda_0 = kh, \quad \lambda_n = k_n h, \quad \bar{\lambda}_s = \bar{k}_s h$$

$$N_0 = \frac{1}{2}(1 + 2\lambda_0/\sinh 2\lambda_0), \quad N_n = \frac{1}{2}(1 + 2\lambda_n/\sin 2\lambda_n), \quad \bar{F}_0(\xi, \eta) = \partial f_0(\xi, \eta)/k\alpha\nu \quad (1.30)$$

(vi) Determination of $f_1, f_2^{(n)}, f_3^{(s)}, \dots$ etc. on the boundary D

Eq. (1.18) (1.19) (1.20) and (1.26) (1.27) (1.28) (1.29) are the relations to determine $f_1, f_2^{(n)}, \dots$ on the boundary.

From Eq. (1.20), $\bar{F}_3^{(s)}(\xi_i, \eta_i)$ is expressed by $f_3^{(s)}(\xi_j, \eta_j)$ as follows:

$$\bar{F}_3^{(s)}(i) = \sum_{j=1}^N M_{ij}^{(s)} f_3^{(s)}(j) \quad \text{where} \quad M_{ij}^{(s)} = \frac{1}{\Delta^{(s)}} \sum_{k=1}^N \gamma_{kj}^{(s)} \Delta_{ki}^{(s)} \quad (1.31)$$

where $\Delta^{(s)}$ is the matrix by $F_{ij}^{(s)}$, $\Delta_{ki}^{(s)}$ is the determinant, given by removing the "k"th row and the "i"th column from $\Delta^{(s)}$ and then multiplying $(-1)^{k+i}$ and $\gamma_{kj}^{(s)} = \delta_{kj} + \bar{A}_{kj}^{(s)}$, δ_{kj} is Kronecker's delta, i.e. $\delta_{kj} = 0 (k \neq j) : = 1 (k = j)$.

Substituting Eq. (1.26) (1.29) into Eq. (1.18) (1.19), and then eliminating $\bar{F}_3^{(s)}$ by Eq. (1.31), we have next linear simultaneous equations in term of $f_3^{(s)}$.

$$\begin{aligned} \sum_{s=1}^N \frac{1}{1 - (\bar{\lambda}_s/\lambda_0)^2} [f_3^{(s)}(i) + \sum_{j=1}^N \bar{A}_{ij} f_3^{(s)}(j) - A_{ij} \sum_{k=1}^N M_{jk}^{(s)} f_3^{(s)}(k)] \\ = -N_0 [f_0(i) + \sum_{j=1}^N \bar{A}_{ij} f_0(j) - A_{ij} \bar{F}_0(j)] \end{aligned} \quad (1.32)$$

$$\begin{aligned} \sum_{s=1}^N \frac{1}{1 + (\bar{\lambda}_s/\lambda_n)^2} [f_3^{(s)}(i) + \sum_{j=1}^N \bar{B}_{ij}^{(n)} f_3^{(s)}(j) - B_{ij}^{(n)} \sum_{k=1}^N M_{jk}^{(s)} f_3^{(s)}(k)] \\ = 0, \quad (n=1, 2, 3, \dots) \end{aligned}$$

Above equations are applied to $i=1, 2, 3, \dots, N$. If we take n and s to n^*

and s^* , respectively, we have $(n^*+1)N$ equations for s^* unknown $f_3^{(s)}$. Therefore, taking $s^*=n^*+1$, all of $f_3^{(s)}$ ($s=1,2,\dots,s^*$) are determined by solving Eq. (1.32) and then $\bar{f}_3^{(s)}$, f_1 , \bar{f}_1 , $f_2^{(n)}$, $\bar{f}_2^{(n)}$ are obtained by Eq. (1.31) (1.26) (1.27) (1.28) (1.29), respectively.

(vii) Determination of $f_1(x,y)$, $f_2^{(n)}(x,y)$ and $f_3^{(s)}(x,y)$

$f_1(x,y)$, $f_2^{(n)}(x,y)$ and $f_3^{(s)}(x,y)$ at any point of fluid region are calculated by Eq. (1.10) (1.12) (1.13) as follows:

$$\begin{aligned}
 f_1(x,y) &= -\frac{1}{2} \sum_{j=1}^N [\bar{A}_{xj} f(j) - A_{xj} \bar{f}(j)], & f_2^{(n)}(x,y) &= -\frac{1}{2} \sum_{j=1}^N [\bar{B}_{xj}^{(n)} f_2^{(n)}(j) - B_{xj}^{(n)} \bar{f}_2^{(n)}(j)] \\
 f_3^{(s)}(x,y) &= \frac{1}{2} \sum_{j=1}^N [\bar{E}_{xj}^{(s)} f_3^{(s)}(j) - E_{xj}^{(s)} \bar{f}_3^{(s)}(j)]
 \end{aligned}
 \tag{1.33}$$

where A_{xj} , \bar{A}_{xj} , ... are those which are given in Eq. (1.21) by replacing (ξ_i, η_i) by (x,y) .

Thus, wave function $\phi_1(x,y,z)$ and $\phi_2(x,y,z)$ are completely determined and the fluid motions are fully made clear.

(viii) Numerical evaluation

A_{ij} and \bar{A}_{ij} in Eq. (1.21) are calculated numerically, after Lee (1971)⁽⁴⁾ in the following way.

$$\begin{aligned}
 R_{ij} &= \sqrt{(\xi_j - \xi_i)^2 + (\eta_j - \eta_i)^2}, & S_j &= \sqrt{(\Delta \xi_j)^2 + (\Delta \eta_j)^2} \\
 \Delta \xi_j &= \frac{1}{2}(\xi_{j+1} - \xi_{j-1}), & \Delta \eta_j &= \frac{1}{2}(\eta_{j+1} - \eta_{j-1})
 \end{aligned}
 \tag{1.34}$$

Noting that when kr tends to zero,

$$H_0^{(1)}(kr) \doteq 1 + 2i(\log \frac{kr}{2} + \gamma) / \pi, \quad H_1^{(1)}(kr) \doteq -2 \frac{i}{\pi} \frac{1}{kr}$$

$\gamma = 0.577216 \dots$ (Euler's constant)

for $j \neq i$, we obtain

$$\begin{aligned}
 A_{ij} &= -\frac{1}{2} H_0^{(1)}(kR_{ij}) k \Delta S_j \\
 \bar{A}_{ij} &= \frac{i}{2} H_1^{(1)}(kR_{ij}) \left(\frac{\xi_j - \xi_i}{R_{ij}} k \Delta \eta_j - \frac{\eta_j - \eta_i}{R_{ij}} k \Delta \xi_j \right)
 \end{aligned}$$

for $j=i$

$$A_{ii} = \frac{1}{\pi} (\gamma - 1 + \log \frac{k \Delta S_i}{4} - i\pi/2) \quad (1.37)$$

$$\bar{A}_{ii} = \frac{1}{2\pi} (\xi_{ss} \eta_{ss} - \xi_{ss} \eta_{ss})_i \Delta S_i$$

where

$$\xi_s = \frac{\xi_{i+1} - \xi_{i-1}}{2\Delta S_i}, \quad \xi_{ss} = \frac{6}{\Delta S_{i+1} + \Delta S_i + \Delta S_{i-1}} \left[\frac{\xi_{i+1} - \xi_i}{\Delta S_{i+1} + \Delta S_i} - \frac{\xi_i - \xi_{i-1}}{\Delta S_i + \Delta S_{i-1}} \right] \quad (1.38)$$

$$\eta_s = \frac{\eta_{i+1} - \eta_{i-1}}{2\Delta S_i}, \quad \eta_{ss} = \frac{6}{\Delta S_{i+1} + \Delta S_i + \Delta S_{i-1}} \left[\frac{\eta_{i+1} - \eta_i}{\Delta S_{i+1} + \Delta S_i} - \frac{\eta_i - \eta_{i-1}}{\Delta S_i + \Delta S_{i-1}} \right]$$

Similarly, other terms in Eq. (1.21) are as follows:

$$B_{ij}^{(n)} = -\frac{1}{\pi} K_0 (k_n R_{ij}) k \Delta S_j, \quad \bar{B}_{ii}^{(n)} = \frac{1}{\pi} (\gamma - 1 + \log \frac{k_n \Delta S_i}{4}) k \Delta S_i$$

$$\bar{B}_{ij}^{(n)} = \frac{1}{\pi} K_1 (k_n R_{ij}) \left(\frac{\xi_j - \xi_i}{R_{ij}} k_n \Delta \eta_j - \frac{\eta_j - \eta_i}{R_{ij}} k_n \Delta \xi_j \right) \quad (1.39)$$

$$E_{ij}^{(s)} = -\frac{i}{2} H_0^{(1)} (\bar{k}_s R_{ij}) k \Delta S_j, \quad \bar{E}_{ii}^{(s)} = \frac{1}{\pi} (\gamma - 1 + \log \frac{\bar{k}_s \Delta S_i}{4} - i\pi/2) k \Delta S_i$$

$$\bar{E}_{ij}^{(s)} = \frac{i}{2} H_0^{(1)} (\bar{k}_s R_{ij}) \left(\frac{\xi_j - \xi_i}{R_{ij}} \bar{k}_s \Delta \eta_j - \frac{\eta_j - \eta_i}{R_{ij}} \bar{k}_s \Delta \xi_j \right) \quad (1.40)$$

$\bar{B}_{ii}^{(n)}$ and $\bar{E}_{ii}^{(s)}$ are the same as \bar{A}_{ii} . And $f_0(j)$ and $\bar{f}_0(j)$ are as follows:

$$f_0(j) = -i \exp\{-ik(\xi_j \cos \omega + \eta_j \sin \omega)\} \quad (1.41)$$

$$\bar{f}_0(j) = \frac{k_j \sin \omega - \Delta \eta_j \cos \omega}{\Delta S_j} \exp\{-ik(\xi_j \cos \omega + \eta_j \sin \omega)\}$$

(ix) Convergence of the infinite series in ϕ_1 and ϕ_2

For the existence of wave function ϕ_1 and ϕ_2 , infinite series in the righthand sides of Eq. (1.2) and (1.7) must be uniformly convergent in x, y, z . It is difficult for the authors to prove the convergence but it is estimated in the following way.

For large value of n in Eq. (1.2), we have

$$k_n h \approx n\pi - \frac{1}{n\pi} \frac{g^2 h}{g} \quad \text{and} \quad \frac{\varphi}{h} f_2^{(n)}(x, y) \frac{\cos k_n(z+h)}{\cos k_n h} = \frac{\varphi}{h} f_2^{(n)}(x, y) \cos k_n z \quad (1.42)$$

Above series is convergent for $0 \leq z \leq h$, if series $\sum_n f_2^{(n)}(x, y)$ is convergent.

While, sequence $B_{xj}^{(n)}$ and $\bar{B}_{xj}^{(n)}$ in Eq. (1.33) are monotonic decrease for increasing n at any point (x, y) , so that if the series $\sum_n f_2^{(n)}(\xi, \eta)$ and $\sum_n \bar{f}_2^{(n)}(\xi, \eta)$ converges, series $\sum_n f_2^{(n)}(x, y)$ also converges. Similarly, if series $\sum_n f_3^{(s)}(\xi, \eta)$ converges, series $\sum_n f_3^{(s)}(x, y) \cdot \cosh k_s(z+h) / \cosh k_s h$ also converges.

We have

$$N_n \approx -\frac{(n\pi)^2}{2\sigma^2 h/g}, \quad \bar{\lambda}_s \approx \frac{\sigma^2 h}{g} \frac{V\mu}{\sigma} \frac{1}{s\pi} + i(s\pi - \frac{1}{s\pi}) \frac{\sigma^2 h}{g} \quad (1.44)$$

for large n and s . Therefore, in Eq. (1.27)

$$\sum_n \sum_s \frac{f_3^{(s)}(\xi, \eta)}{N_n \{1 + (\bar{\lambda}_s / \lambda_n)^2\}} \approx -\frac{2\alpha}{\pi^2} \frac{\sigma^2 h}{g} \sum_n \sum_s \frac{f_3^{(s)}(\xi, \eta)}{n^2 - s^2 + 2i \frac{1}{2} \frac{V\mu}{\sigma} \sigma^2 h/g} \quad (1.45)$$

Above series are convergent, if series $\sum_s f_3^{(s)}(\xi, \eta)$ converges, and then $\sum_n f_2^{(n)}(\xi, \eta)$ converges.

Moreover, from Eq. (1.40), $E_{ij}^{(s)} \ll E_{ii}^{(s)}$ and $\bar{E}_{ij}^{(s)} \ll \bar{E}_{ii}^{(s)}$ for large s . Therefore, Eq. (1.20) approaches to the following equation for large s .

$$(1 - \bar{E}_{ii}^{(s)}) f_3^{(s)}(i) + E_{ii}^{(s)} \bar{f}_3^{(s)}(i) = 0,$$

from which

$$\bar{f}_3^{(s)}(i) = -\frac{1 - \bar{E}_{ii}^{(s)}}{E_{ii}^{(s)}} f_3^{(s)}(i) \quad (1.46)$$

where $\bar{E}_{ii}^{(s)}$ is independent on s and $E_{ii}^{(s)}$ is approximated as follows:

$$E_{ii}^{(s)} \approx \frac{k\Delta S_i}{\pi} \{-1 + i(\frac{s\pi\Delta S_i}{4h} - \pi/2)\} \quad (1.47)$$

$E_{ii}^{(s)}$ increases with increasing s , so that from Eq. (1.46), $\sum_s \bar{f}_3^{(s)}(\xi, \eta)$ converges, if $\sum_s f_3^{(s)}(\xi, \eta)$ converges.

Thus, if $\sum_s f_3^{(s)}(\xi, \eta)$ converges, $\sum_s \bar{f}_3^{(s)}(\xi, \eta)$, $\sum_n f_2^{(n)}(\xi, \eta)$ and $\sum_n \bar{f}_2^{(n)}(\xi, \eta)$ are convergent, and wave functions $\phi_1(x, y, z)$ and $\phi_2(x, y, z)$ exist. But it is difficult to prove mathematically the convergency of $\sum_s f_3^{(s)}(\xi, \eta)$ and is estimated numerically, as shown in later example.

In practical calculations, infinite series are replaced by finite series,

Hence, the accuracy of calculation should be tested by the agreement of both sides of Eq. (1.24) (1.25) for any value of z at any point (ξ, η) .

(x) Wave height distribution and wave forces to breakwater

Wave profiles ζ_I and ζ_{II} at any point in outer and inner regions are given by following equations.

$$\zeta_I = i\zeta_0\phi_1(x, y, z)e^{-i\sigma t} \quad , \quad \zeta_{II} = i\zeta_0\phi_2(x, y, z)e^{-i\sigma t} \quad (1.48)$$

And the ratios of wave height in both regions to incident wave height $K_d^{(1)}$ and $K_d^{(2)}$ are calculated as follows:

$$K_d^{(1)} = |f_0(x, y) + f_1(x, y) + \sum_{n=1}^{\infty} f_2^{(n)}(x, y)| \quad , \quad K_d^{(2)} = \left| \frac{1+i\mu V/\sigma}{V} \sum_{s=1}^{\infty} f_3^{(s)}(x, y) \right| \quad (1.49)$$

Wave forces F_x and F_y to breakwater in positive x and y directions are calculated as follows:

$$\frac{F_x}{\rho g \zeta_0 h^2} = -i e^{-i\sigma t} \frac{\sigma^2 h}{g} \frac{(1+i\mu V/\sigma)^2}{V} \sum_{s=1}^{\infty} \sum_{j=1}^N \frac{f_3^{(s)}(j)}{\lambda_0(\bar{\lambda}_s)^2} k \Delta \eta_j \quad (1.50)$$

$$\frac{F_y}{\rho g \zeta_0 h^2} = i e^{-i\sigma t} \frac{\sigma^2 h}{g} \frac{(1+i\mu V/\sigma)^2}{V} \sum_{s=1}^{\infty} \sum_{j=1}^N \frac{f_3^{(s)}(j)}{\lambda_0(\bar{\lambda}_s)^2} k \Delta \xi_j \quad (1.51)$$

II Analysis for Impermeable Breakwater

For impermeable breakwater, the scattering terms $f_2^{(n)}(x, y)$ in Eq. (1.2) vanish identically and wave function $\phi_1(x, y, z)$ becomes simple as follows:

$$\phi_1(x, y, z) = \frac{g\zeta_0}{\sigma} [f_0(x, y) + f_1(x, y)] \frac{\cosh k(z+h)}{\cosh kh} \quad (2.1)$$

On the boundary D , fluid velocity normal to D should vanish, so that

$$\partial\phi_1(\xi, \eta, z)/\partial\nu = 0 \quad , \quad \text{and so} \quad \partial f_1(\xi, \eta)/\partial\nu = -\partial f_0(\xi, \eta)/\partial\nu \quad (2.2)$$

Substituting this relation into Eq. (1.14), we have next integral

equation to determine $f_1(\xi, \eta)$

$$f_1(\xi', \eta') + \int_D f_1(\xi, \eta) \frac{\partial}{\partial \nu} \left(-\frac{1}{2} H_0^{(1)}(kR) \right) ds = - \int_D \left(-\frac{1}{2} k H_0^{(1)}(kR) \right) \bar{f}_0(\xi, \eta) ds \quad (2.3)$$

from which, f_1 is determined by the following linear equations.

$$f_1(i) + \sum_{j=1}^N \bar{A}_{ij} f_1(j) = - \sum_{j=1}^N A_{ij} \bar{f}_0(j) \quad , \quad (i=1, 2, 3, \dots, N) \quad (2.4)$$

And the first equation in Eq. (1.33), $f_1(x, y)$ and hence $\phi_1(x, y, z)$ are determined.

Distribution of wave height ratios and wave forces to breakwater are calculated by the following equations.

$$K_d = |f_0(x, y) + f_1(x, y)| \quad (2.5)$$

$$\frac{F_x}{\rho g \zeta_0 h^2} = -ie^{-i\omega t} \frac{\sigma^2 h}{g} \frac{1}{\lambda_0^3} \sum_{j=1}^N [f_0(x, y) + f_1(x, y)] k \Delta \eta_j \quad (2.6)$$

$$\frac{F_y}{\rho g \zeta_0 h^2} = ie^{-i\omega t} \frac{\sigma^2 h}{g} \frac{1}{\lambda_0^3} \sum_{j=1}^N [f_0(x, y) + f_1(x, y)] k \Delta \xi_j$$

III Numerical calculation

Here, breakwaters of elliptic and rectangular shape, where x and y radii are $2a$ and $2b$, and x -side and y -side are $2a$ and $2b$, respectively, calculate the case when $a/b=0.2$, $b/h=2.5$, for wave of $\sigma^2 h/g=0.5$, $kh=0.772$ ($kb=1.93$).

In general, it is desired to make distance ΔS_j between successive calculation points in the boundary be shorter than about one eighth of wave length. Hence, in these calculations, twenty calculation points are distributed along the boundary as shown in Fig.2 where the largest distance between successive points is about $0.13L$ (L : wave length).

(i) Convergence of the series

As an example, taking $n^* = 3, s^* = 4$, the numerical values of $f_1(j), f_2^{(n)}(j)$ and $f_3^{(s)}(j)$ at every calculation points are shown in Table-1 for elliptic

breakwater of $V=0.5$, $\mu V/\sigma=1.0$ for wave of $\sigma^2 h/g=0.5$, $\omega=0^\circ$. (For the case of $\omega=0^\circ$, values at symmetrical points with respect to x axis are the same, so that, values at $j=11\sim 19$ are the same as those at $j=1\sim 9$, respectively.)

From the results, it is found that the convergence of the series discussed in II(vii) is satisfactory and $n^*=3, s^*=4$ are sufficient for practical calculation of this case.

(ii) Exactness of calculation

The exactness of calculation are determined numerically by testing how accurately the continuity conditions Eq.(1.24) and (1.25) are satisfied. Table-2 shows the numerical comparisons of both sides of Eq.(1.24) and(1.25) at depth of $z/h= 0.-0.2,-0.4,\dots, -1.0$ at point $j=10$ and 15 in above case. From the results, it is found that the exactness of calculation is sufficient.

(iii) Wave height distribution

Fig.3~6 are calculated wave height distributions by Eq.(1.49) for permeable breakwater with $V=0.5$, $\mu V/\sigma =1.0$ and by Eq.(2.5) for impermeable breakwater, where the former are shown by broken curves and latter by full curves.

Fig. 7~10 are those for the case when $b/h=2.5(kb=1.93)$, $a/b=0.5$, $\sigma^2 h/g=0.5(kh=0.772)$ and $V=0.5$, $\mu V/\sigma=1.0$.

From these distributions, it can be seen that:

- (a) The differences between rectangular and elliptic breakwater arise from the apexes of rectangle and clearly appear for $\omega=0^\circ$ and almost disappear for $\omega=90^\circ$.
- (b) The longer becomes the breakwater, the more clearly appears the standing wave in front of breakwater, for $\omega=0^\circ$ in case of $b/h=1.0$, the standing wave almost disappears.
- (c) The wave height in front of permeable breakwater is always smaller than that of impermeable one. And wave height behind permeable breakwater is smaller than the one behind impermeable breakwater for the case of short breakwater but is adverse for the case of long breakwater. This is due to fact that for short breakwater, waves behind it are mainly diffracted waves and behind permeable breakwater they are smaller than those behind impermeable one, and for long breakwater, waves behind permeable one are mainly transmitted waves through breakwater but those behind impermeable one are mainly diffracted waves and become smaller for longer breakwater.

(iv) Wave Forces

Calculated wave forces by (1.50), (1.51) and (2.6) are as shown in Table-3.

(v) Comparisons with experiments

For comparisons of analysis with experiments, rectangular and elliptic breakwater models are placed in wave channel of length 25m, width 1m and depth 0.6m with flap-type wave generator as shown in Fig.11.

Impermeable models are made of concrete and permeable models are of wire screen filled by small concrete blocks, of which the average void is 0.40, and $b/h=1.0$, $a/b=0.5$. The water depth is 20cm, wave period is kept constant as 1.28 sec. ($\sigma^2 h/g=0.5$)

Considering the effect of reflection by channel walls, wave height distributions are calculated, taking $V=0.50$, $\mu/\sigma=2.0$, for the boundary conditions as shown in fig.11, that is, at imaginary boundary W_2 and W_4 far from breakwater waves progress from right to left without reflection waves and at channel walls W_1 and W_3 , normal velocity of fluid motion vanishes.

And under the same conditions, wave heights are measured. The results of calculations and experiments are shown in Fig. 12~15, where left and right parts are by calculations and experiments, respectively. From these figures, it is found that results of calculation agree fairly well with those of experiments.

IV Conclusions

In above calculations, we assumed $V=0.5$, $\mu/\sigma=2.0$ and found that theory and experiments are in good agreement. In this analysis V and μ/σ are interpreted as virtual quantities related to void and fluid resistance of breakwater. Hence they are not necessarily the same as the actual values, but are to be selected so as to obtain agreement of theory and experiments.

The method of analysis described in this paper can be applied to the calculations not only for elliptical and rectangular shapes but also for arbitrary shapes. And the same principle is available to the analysis of permeable quay wall, and also of fixed semi-immersed, of submerged cylinders.

Reference

- (1) Takeshi IJIMA, Yasuhiko EGUCHI, Akira KOBAYASHI (1971):
"Theory and Experiment on Permeable Breakwater and Quay Wall", Proc. 18th Conf. Coast Eng. Japan (in Japanese)
- (2) John, Fritz (1950): "On the motion of Floating Bodies II", Communications on Pure and Applied Mathematics, Vol. III No. 1-4, pp. 45-100
- (3) same as (1)
- (4) Lee, Jiin-Jen (1970): "Wave-induced Oscillations in Harbors of Arbitrary Shape", Calif. Inst. for Technology

Table 1
Successive values of f_1 , $f_2^{(n)}$, and $f_3^{(s)}$ for $\sigma^2 h/g=0.5$

j	f_1	$f_2(1)$	$f_2(2)$	$f_2(3)$
20	-0.5171 -0.1911i	0.0105 +0.0168i	-0.0376 +0.0191i	-0.0002 -0.0001i
1	-0.3172 -0.0438i	0.0066 +0.0171i	-0.0027 +0.0043i	-0.0010 +0.0006i
2	-0.2138 +0.0105i	-0.0230 -0.0074i	0.0007 +0.0049i	0.0010 +0.0020i
3	-0.0780 -0.0137i	-0.0127 -0.0010i	0.0018 +0.0037i	0.0012 +0.0017i
4	-0.0101 -0.0317i	-0.1112 -0.0012i	0.0018 +0.0029i	0.0011 +0.0014i
5	0.0504 -0.0589i	-0.0123 -0.0032i	0.0016 +0.0027i	0.0011 +0.0012i
6	0.1107 -0.0934i	-0.0166 -0.0069i	0.0015 +0.0032i	0.0013 +0.0013i
7	0.1550 -0.1113i	-0.0259 -0.0146i	0.0009 +0.0044i	0.0016 +0.0013i
8	0.2485 -0.1828i	-0.0974 -0.0710i	-0.0150 +0.0123i	0.0028 +0.0011i
9	0.3379 -0.2024i	0.0195 +0.0155i	-0.0161 +0.0127i	0.0029 -0.0005i
10	0.4492 -0.2315i	0.0357 +0.0003i	0.0094 -0.0042i	0.0060 -0.0044i

j	$f_3(1)$	$f_3(2)$	$f_3(3)$	$f_3(4)$
20	0.1560 -0.0287i	0.0022 -0.0157i	-0.0060 +0.0101i	-0.0004 -0.0017i
1	0.2331 -0.0647i	-0.0029 -0.0227i	-0.0021 -0.0042i	-0.0012 -0.0022i
2	0.2640 -0.0971i	-0.0203 -0.0247i	-0.0020 -0.0050i	-0.0008 -0.0024i
3	0.2834 -0.1605i	-0.0233 -0.0273i	-0.0038 -0.0060i	-0.0016 -0.0027i
4	0.2917 -0.1939i	-0.0267 -0.0285i	-0.0049 -0.0063i	-0.0021 -0.0028i
5	0.2937 -0.2299i	-0.0315 -0.0286i	-0.0059 -0.0062i	-0.0025 -0.0028i
6	0.2927 -0.2677i	-0.0377 -0.0282i	-0.0068 -0.0058i	-0.0029 -0.0027i
7	0.2916 -0.2948i	-0.0450 -0.0275i	-0.0073 -0.0050i	-0.0031 -0.0026i
8	0.2821 -0.3610i	-0.0848 -0.0223i	-0.0108 +0.0026i	-0.0034 -0.0023i
9	0.2825 -0.3998i	-0.0377 -0.0296i	-0.0122 +0.0013i	-0.0043 -0.0033i
10	0.2775 -0.4542i	-0.0431 -0.0366i	-0.0117 -0.0090i	-0.0037 -0.0049i

Table 2

Numerical check on the boundary conditions

(i) Continuity of fluid pressure

j	z/h	Region I	Region II
10	0.0	0.3821 +0.2298i	0.3755 +0.2317i
	-0.2	0.3716 +0.1859i	0.3738 +0.1823i
	-0.4	0.3795 +0.1442i	0.3786 +0.1464i
	-0.6	0.3542 +0.1264i	0.3525 +0.1261i
	-0.8	0.2944 +0.1348i	0.2950 +0.1338i
	-1.0	0.2637 +0.1432i	0.2628 +0.1447i
15	0.0	1.0487 -0.0582i	1.0421 -0.0282i
	-0.2	0.9485 -0.0562i	0.9479 -0.0559i
	-0.4	0.8825 -0.0552i	0.8828 -0.0483i
	-0.6	0.8428 -0.0469i	0.8428 -0.0477i
	-0.8	0.8209 -0.0415i	0.8207 -0.0443i
	-1.0	0.8131 -0.0402i	0.8134 -0.0360i

(ii) Continuity of fluid velocity

10	0.0	-0.0746 +0.0076i	-0.0750 +0.0052i
	-0.2	-0.0362 +0.0688i	-0.0362 +0.0670i
	-0.4	-0.0154 +0.2579i	-0.0153 +0.2575i
	-0.6	-0.1214 +0.5515i	-0.1214 +0.5515i
	-0.8	-0.3093 +0.8383i	-0.3094 +0.8386i
	-1.0	-0.4047 +0.9596i	-0.4047 +0.9592i
15	0.0	0.0415 -0.0359i	0.0428 -0.0349i
	-0.2	0.0630 +0.0020i	0.0625 +0.0018i
	-0.4	0.0725 +0.0372i	0.0748 +0.0373i
	-0.6	0.0326 +0.0200i	0.0326 +0.0199i
	-0.8	0.0087 +0.0104i	0.0085 +0.0104i
	-1.0	0.0112 +0.0177i	0.0115 +0.0177i

Table 3
Calculated Results for Wave Forces

Shape	Ellipse			Rectangle			Remarks	
Cross-section Area	πab			$4ab$				
Angle of Incident ω	0°	45°	90°	0°	45°	90°		
$\sigma^2 h/g = 0.5$, $kb = 1.93$								
$\frac{F_x}{\rho g \zeta_0 h^2}$	a/b=	9.146	5.374	0.0	9.641	5.447	0.0	Imperm.
	0.2	4.208	2.427	0.0	4.802	2.561	0.0	Perm.
$\frac{F_x}{\rho g \zeta_0 h^2}$	a/b=	8.562	5.074	0.0	9.184	5.564	0.0	Imperm.
	0.5	6.184	3.626	0.0	6.956	3.784	0.0	Perm.
$\frac{F_y}{\rho g \zeta_0 h^2}$	a/b=	0.0	1.371	1.508	0.0	1.644	1.417	Imperm.
	0.2	0.0	1.280	1.411	0.0	1.736	1.604	Perm.
$\frac{F_y}{\rho g \zeta_0 h^2}$	a/b=	0.0	3.210	3.673	0.0	3.973	3.466	Imperm.
	0.5	0.0	2.894	3.273	0.0	3.433	3.403	Perm.
$\sigma^2 h/g = 1.0$, $kb = 3.00$								
$\frac{F_x}{\rho g \zeta_0 h^2}$	a/b=	6.431	2.773	0.0	6.774	2.534	0.0	Imperm.
	0.2	4.033	1.595	0.0	4.546	1.400	0.0	Perm.
$\frac{F_x}{\rho g \zeta_0 h^2}$	a/b=	6.571	2.418	0.0	6.952	2.175	0.0	Imperm.
	0.5	5.023	1.821	0.0	5.651	1.247	0.0	Perm.
$\frac{F_y}{\rho g \zeta_0 h^2}$	a/b=	0.0	1.148	0.687	0.0	1.122	0.479	Imperm.
	0.2	0.0	1.002	0.552	0.0	1.103	0.404	Perm.
$\frac{F_y}{\rho g \zeta_0 h^2}$	a/b=	0.0	2.560	1.797	0.0	2.752	2.893	Imperm.
	0.5	0.0	2.082	1.412	0.0	2.117	1.948	Perm.

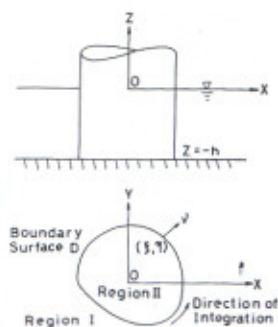


Fig.1 Definition Sketch

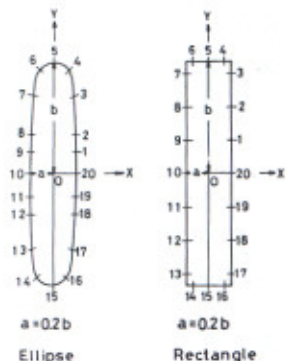


Fig.2 Distribution of Calculation Points

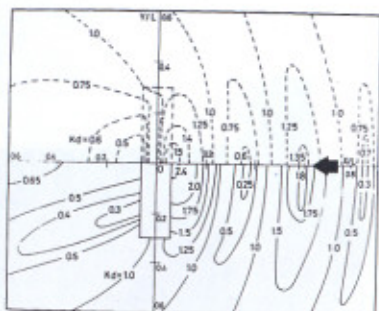


Fig.3 Distribution of Kd for Rectangle

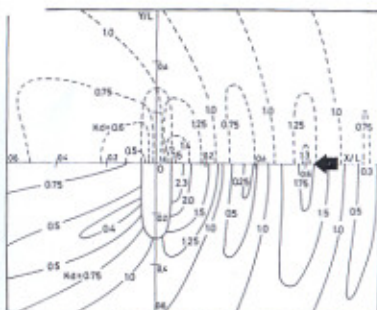


Fig.4 Distribution of Kd for Ellipse

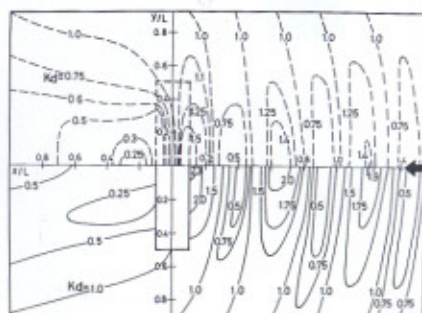


Fig.5 Distribution of Kd for Rectangle

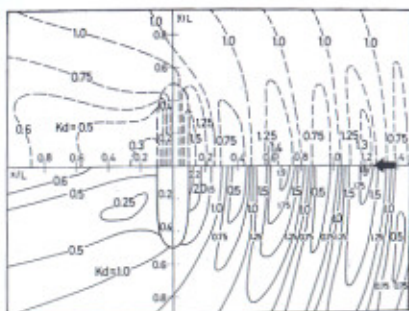
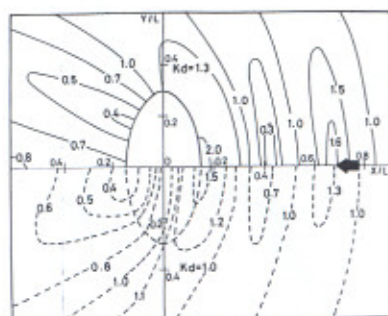
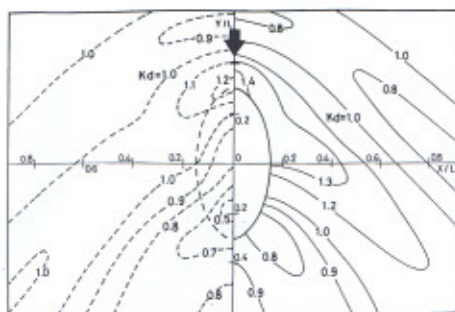


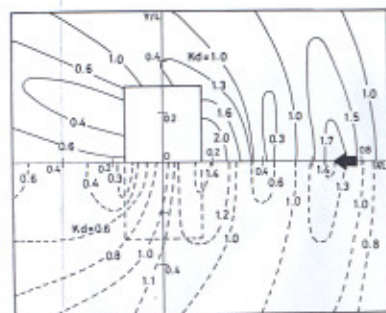
Fig.6 Distribution of Kd for Ellipse



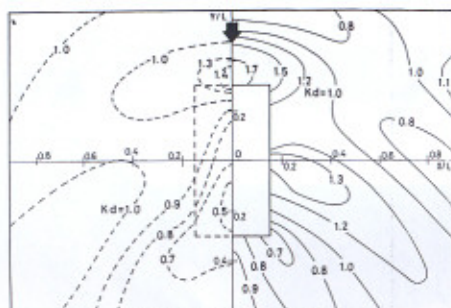
$\sigma^2/hg=0.5$ $Kb=1.93$ $b/h=2.5$ $a/b=0.5$
Fig. 7 Distribution of K_d for Ellipse



$\sigma^2/hg=0.5$ $Kb=1.93$ $b/h=2.5$ $a/b=0.5$
Fig. 8 Distribution of K_d for Ellipse



$\sigma^2/hg=0.5$ $Kb=1.93$ $b/h=2.5$ $a/b=0.5$
Fig. 9 Distribution of K_d for Rectangle



$\sigma^2/hg=0.5$ $Kb=1.93$ $b/h=2.5$ $a/b=0.5$
Fig. 10 Distribution of K_d for Rectangle

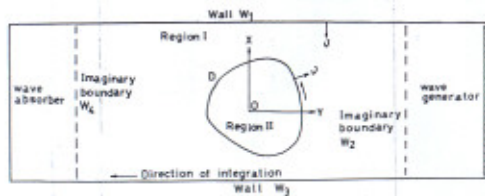


Fig. 11 Definition Sketch

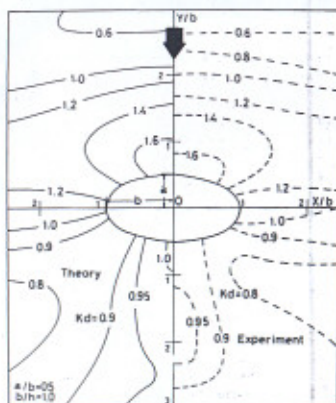


Fig. 12 $\sigma^2/hg=0.5$, Distribution of K_d for Impermeable Ellipse

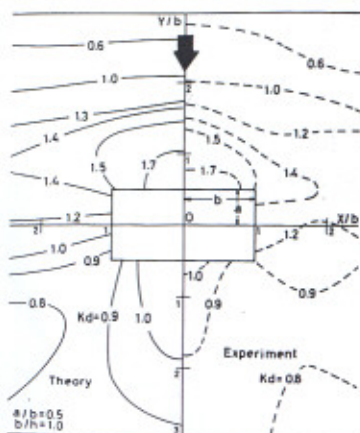


Fig. 13 $\sigma^2 h/g=0.5$, Distribution of Kd for Impermeable Rectangle

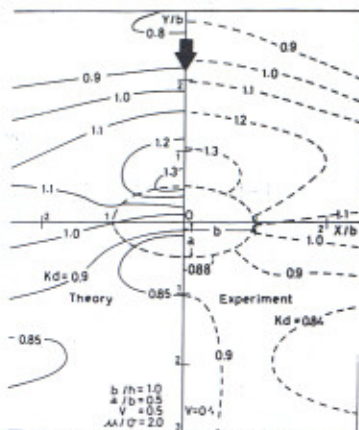


Fig. 14 $\sigma^2 h/g=0.5$, Distribution of Kd for Permeable Ellipse

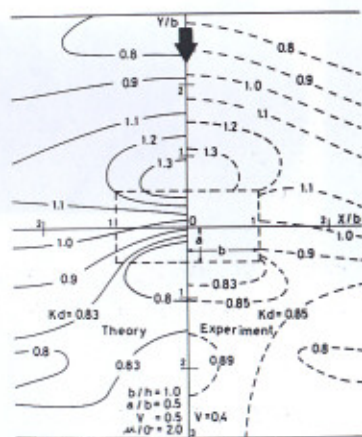


Fig. 15 $\sigma^2 h/g=0.5$, Distribution of Kd for Permeable Rectangle